Analytical Evaluation of Signal to Noise Ratios for SiPM and APD in dToF LiDAR Applications

AND90257/D

Introduction

Light Detection and Ranging, *LiDAR* is a critical system for advanced driver assistance systems, *ADAS,* and autonomous driving, *AD,* vehicles, robotic mobility, and industrial automation. The signal to noise ratio, *SNR,* of the LiDAR system is a key parameter that limits the LiDAR detection probability, particularly at long distances.

The *SNR* calculation method depends on sensor selection; this application note presents the analytical calculation of *SNR* for SiPM, and for Si and InGaAs APD sensors in a direct time of flight, *dToF* LiDAR application.

We analyze *SNR* for APD−based systems operating at 2 wavelengths, 905 nm and 1550 nm, and a SiPM−based LiDAR operating at 905 nm.

The LiDAR system specifications employed for the analysis are typical of today's Level 2 or Level 3 automotive systems.

The effect of varying the system optical parameters is also explored since angular resolution and lens aperture (i.e. lens diameter) can impact the *SNR* performance in a different way depending on sensor choice.

The following sections provide:

1. Power calculations for light signal and background ambient noise
2. The *SNR* analytical calculation applied to APDs operating at 905 nm and 1550 nm and to a SiPM from onsemi at 905 nm. For SiPM the calculations are verified using waveform simulation
3. Analysis of the effect of sensor choice, optical parameters, and readout electronics on *SNR*
4. Discussion of system level design tradeoffs considering the results of the *SNR* analysis

Ambient Light Background and Return Signal Calculations

The background optical power from ambient light reaching the sensor can be calculated as [1]:

$$P_B = \frac{1}{2\pi \cdot d^2} \cdot \Phi_{amb.} \cdot A_{FoV} \cdot \eta \cdot \varepsilon_{RX} \cdot A_{aperture} \qquad \text{(eq. 1)}$$

where d is target distance, ε_{RX}, is receiver optics efficiency, $A_{aperture}$ is receiving lens aperture, which is calculated from lens diameter D_{lens} as $A_{aperture} = \pi\,(D_{lens}{}^2 / 4)$, η is target reflectivity, A_{FoV} is the field of view area at distance d, which can be calculated as:

$$A_{FoV} = 4d^2 \cdot \tan\left(\frac{AoV_x}{2}\right) \cdot \tan\left(\frac{AoV_y}{2}\right) \qquad \text{(eq. 2)}$$

where AoV_x and AoV_y are the sensor horizontal and vertical angle of view, $\Phi_{amb.}$ is ambient light power per unit area, which can be calculated from the solar irradiance spectrum as:

$$\Phi_{amb.} = \int_{\lambda-\Delta\lambda/2}^{\lambda+\Delta\lambda/2} I_{sun}(x)dx \qquad \text{(eq. 3)}$$

where λ is laser wavelength and $\Delta\lambda$ is the bandpass filter width and I_{sun} is spectral solar irradiance. By combining Eq.1, Eq.2 and Eq.3 the $P_{B.}$ can be calculated as:

$$P_B = \frac{1}{2} \cdot \tan\left(\frac{AoV_x}{2}\right) \cdot \tan\left(\frac{AoV_y}{2}\right) \cdot \eta \cdot D_{lens}^2 \cdot \int_{\lambda-\Delta\lambda/2}^{\lambda+\Delta\lambda/2} I_{sun}(x)dx = f\,(\eta, AoV, D_{lens}, \lambda, \Delta\lambda) \qquad \text{(eq. 4)}$$

We can observe from above that the background light power is a function of one condition parameter: target reflectivity, η, and four design parameters: LiDAR angle of view, lens diameter, laser wavelength and bandpass filter width. Φ_{amb} can also be expressed as a photon rate:

$$F_{amb.} = \frac{\Phi_{amb.}}{hc/\lambda} \qquad \text{(eq. 5)}$$

where c is speed of light in vacuum (2.997E8 m/s) and h is Planck's constant (6.626E−10 J/Hz). Assuming a fixed η, AoV and D_{lens}, the ambient light level at different λ may be compared as a function of $\Delta\lambda$. From Table 1. we can observe that the 1550 nm system receives 2.6 times lower background ambient power, however the number of incident photons per second is only 1.6 times smaller due to the difference in photon energy between 905 nm and 1550 nm.

Table 1. COMPARISON OF AMBIENT BACKGROUND POWER IN 905 nm AND 1550 nm SYSTEMS FOR DIFFERENT BANDPASS FILTER WIDTHS

$\Delta\lambda$ nm	Φ_{amb} W/m^2		$\Phi_{amb.}(905)$ / $\Phi_{amb.}(1550)$	$F_{amb.}(905)$ / $F_{amb.}(1550)$
	905 nm	1550 nm		
6	4.42	1.62	2.72	1.59
10	7.07	2.71	2.61	1.52
20	13.81	5.40	2.56	1.49
50	37.72	13.27	2.84	1.66
80	56.34	20.81	2.70	1.57

Assuming a Lambertian target where the laser spot is within the sensor *AoV* and is smaller than the target, the intensity of the return laser pulse at the sensor can be calculated as:

$$P_S = \frac{1}{2\pi \cdot d^2} \cdot P_{laser} \cdot \varepsilon_{RX} \cdot \varepsilon_{TX} \cdot \eta \cdot A_{aperture} \quad \text{(eq. 6)}$$

where P_{laser} is the initial laser power and ε_{TX}, is emitter optics efficiency.

To illustrate the relationship between P_B, P_S and *SNR* in practice, a generic LiDAR system is employed. The system level specifications and target performance are presented in Table 2 with three optional values for AoV_x and AoV_y which define the system resolution. D_{lens} is variable such that a different optical aperture may be chosen for optimal performance with the detector and wavelength of choice. The ambient light flux is set to 100klux, while target reflectivity is set to 10% as this represents the most challenging condition for *SNR* in the LiDAR application.

Table 2. TYPICAL LiDAR SYSTEM SPECIFICATIONS USED FOR *SNR* ANALYSIS

Condition	Test System		
	#1	#2	#3
FoV (H×V)	120° × 40°		
AoV_x	1°	0.1°	0.05°
AoV_y	1°	0.1°	0.05°
ε_{RX}	90 %		
ε_{TX}	90 %		
D_{lens}	from 1 to 50 mm		
λ	905 or 1550 nm		
$\Delta\lambda$	50 nm		
t_{laser}	10 ns		
N_{shots}	1		
P_{laser}	100 W		
Target Distance d	50 m, 200 m		
Target reflectivity η	10%		
Ambient Light Flux	100 kLux		

Both signal (Eq.6) and background (Eq.4) powers are functions of $A_{aperture} = f(D_{lens})$. Therefore, P_B and P_S were calculated for different D_{lens} values from 1mm up to 50 mm and plotted in Figure 1 for 200 m and 50 m targets. We can observe that a system with a larger aperture collects more return laser light power, P_S, however the background power, P_B in such a system is higher too. P_B might be decreased, without compromising P_S, by reducing the filter bandpass width, $\Delta\lambda$, and sensor angle of view AoV_x, AoV_y. If $\Delta\lambda$, and *AoV* are otherwise constrained by system design choices, a large D_{lens} is recommended for LiDAR systems equipped with low light sensitivity detector, while for systems equipped with high light sensitivity a small D_{lens} size is preferable.

Signal to Noise Calculation for Si and InGaAs APDs

The Signal to Noise Ratio *SNR* of an APD−based LiDAR system can be calculated [2] as:

$$SNR_{APD} = \frac{\sqrt{N_{shots} \times R_O^2 \times P_S^2}}{\sqrt{2eB_n \times F \times (R_O \cdot P_S + R_O \cdot P_B + I_D) + \frac{B_N}{M^2}\left(\frac{4k_BT}{R_f} + \frac{<V_{amp}>^2}{R_f^2}\right)}} \quad \text{(eq. 7)}$$

where N_{shots} is the number of dToF measurements per point, R_0 is APD responsivity without multiplication*, *e* is electron charge, B_N is noise bandwidth (frequency at which amplifier gain is equal to 0 dB), *F* is APD excess noise factor, I_D is APD dark current, *M* is APD multiplication factor or Gain, *T* is temperature in K, $<V_{amp}>$ is amplifier input voltage noise density and R_f is feedback resistance.

*Typically, the responsivity after multiplication $R = R_0 \times M$ is presented in APD datasheets

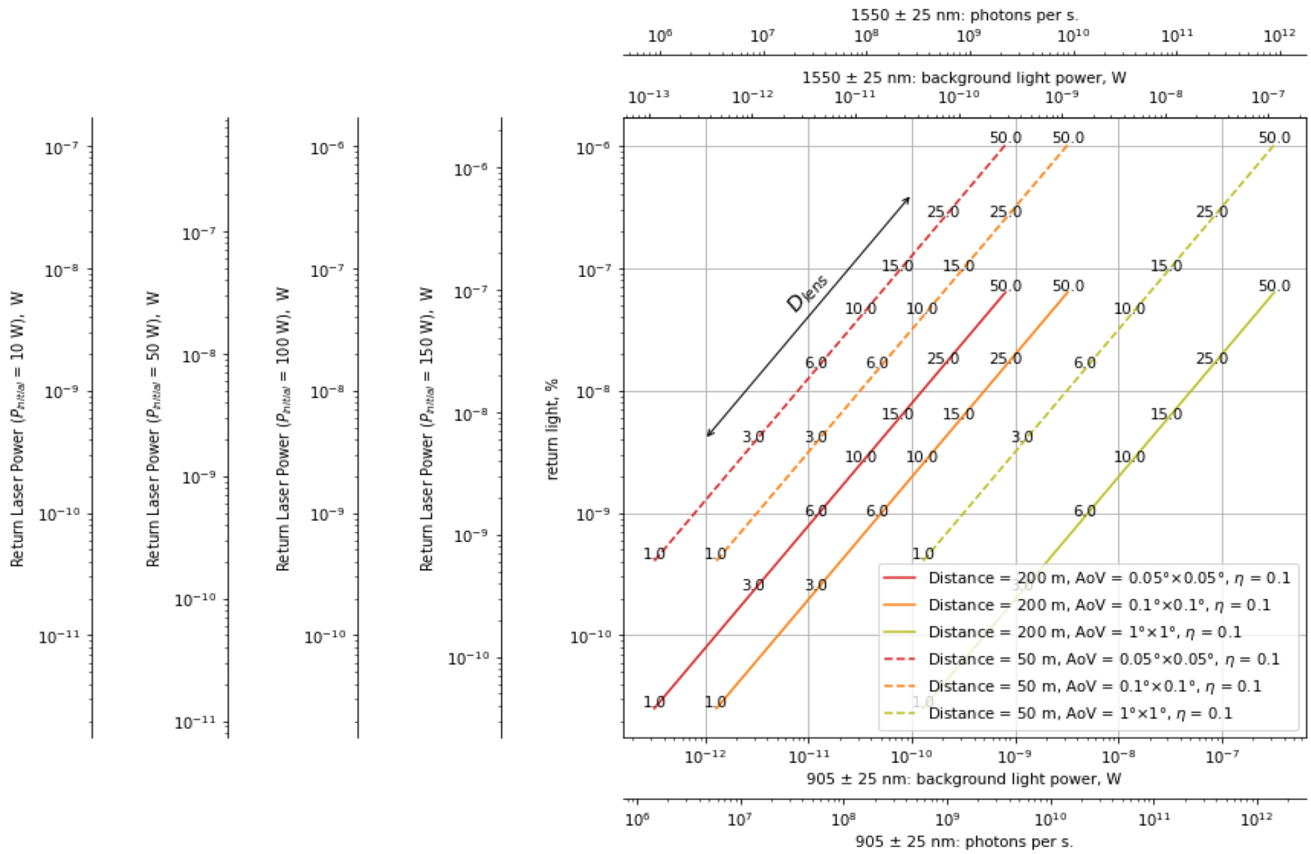

Figure 1. Return Laser Power (expressed in percentage and Watts for initial laser power of 150, 100, 50 and 10 W) as a Function of Background Light Power (expressed in Watts and photons per second) for 905 and 1550 nm Systems. Results presented at different D_{lens} and *AoV* Values and for two Target Distances of 200 m and 50 m.

Table 3. APD (Si AND InGaAs) AND SiPM PARAMETERS USED FOR *SNR* CALCULATIONS

	APD		onsemi SiPM
	Si	InGaAs	
λ	905 nm	1550 nm	905 nm
Δλ	50 nm		
QE	55 %	72 %	N/A
PDE	N/A	N/A	30%
R_0	0.4	0.9	N/A
M or G	100	30	1e6
F	4	7	1.35
I_D	50 pA	150 nA	2 pA
DCR	N/A	N/A	1 MHz/mm^2
N_{cells}	N/A	N/A	2400
P_{XT}	N/A	N/A	15%
$\tau_{dead.}$	N/A	N/A	14 ns
B_N	1 MHz		
R_f	10 kΩ		
<V_{amp}>	28 nV/√Hz		

SNR was calculated for one Si APD at 905 nm and one InGaAs APD at 1550 nm. The InGaAs APD has smaller bandgap energy with respect to Si making it sensitive to longer wavelengths. However, due to shorter bandgap energy InGaAs devices have higher I_D (for the same active area) compared to Si APDs. Moreover, the Si process is more advanced and purer than InGaAs which leads to even lower I_D in the Si sensor. I_D is an important APD parameter which limits the maximum APD multiplication, M, which limits responsivity $R=R_0 \times M$. The Si and InGaAs APD parameters are listed in Table 3. In the system model it is assumed the APD is connected to a transimpedance amplifier with noise bandwidth B_N = 1 MHz and feedback resistor R_f of 10 kΩ.

The *SNR* as a function of P_S and P_B for Si and InGaAs APDs was calculated from Eq.7 and is plotted in Figure 6. The expected values of P_S and P_B are plotted for a laser with initial power of 100 W by white ($AoV_x \times AoV_y = 1° \times 1°$), grey ($AoV_x \times AoV_y = 0.1° \times 0.1°$) and black ($AoV_x \times AoV_y = 0.05° \times 0.05°$) lines, for a target at 200 m distance and with different D_{lens} from 1 to 50 mm. The locations at which *SNR* = 10 are highlighted by dashed red lines.

Signal to Noise Calculation for SiPM Device

A SiPM is a parallel array of microcells where each microcell is composed of a Single Photon Avalanche Diode, SPAD, connected in series with a quenching resistor [3]. Each SiPM microcell works as a binary device producing a short uniform pulse each time a photon is detected. The SiPM generates an analog output signal, which is the sum of signals from all microcells. The SiPM parameters used for *SNR* calculation are presented in Table 3.

For SiPM, the detected noise floor can be expressed in terms of average number [1] of busy microcells due to ambient light:

$$N_{amb} = N_{cells} \cdot \left(1 - e^{-\left(\frac{P_B}{hc/\lambda} \cdot PDE + DCR\right) \frac{\tau_{dead}}{N_{cells}/(1 - <XT>)}} \right) \tag{eq. 8}$$

where *PDE* is SiPM photon detection efficiency, τ_{dead} is dead time and N_{cells} is number of microcells, *DCR* is SiPM dark count rate and $<XT>$ is an average number of crosstalk events per single avalanche, calculated from SiPM crosstalk probability P_{XT} as [4]:

$$< XT > = -\ln(1 - P_{XT}) \tag{eq. 9}$$

The detected return laser signal can be calculated as a number of microcells, N_{laser}, firing due to laser photons:

$$N_{laser} = (N_{cells} - N_{amb}) \cdot \left(1 - e^{-\left(\frac{P_S}{hc/\lambda} \cdot PDE + DCR\right) \frac{t_{laser}}{N_{cells}/(1 - <XT>)}} \right) \tag{eq. 10}$$

where t_{laser} is the laser pulse width.

The *SNR* for SiPM devices can be calculated from the number of fired microcells as:

$$SNR_{SiPM} = \sqrt{N_{shots}} \frac{N_{laser}}{\sqrt{N_{amb} + N^2_{elec.}}} \tag{eq. 11}$$

where $N_{elec.}$ is the number of microcells occupied due to electronic noise:

$$N^2_{elec.} = \left(\frac{\tau_{dead}}{e \times G}\right)^2 \times B_N \times \left(\frac{4k_BT}{R_f} + \frac{< V_{amp} >^2}{R_f^2}\right) \tag{eq. 12}$$

The *SNR* for SiPM, as a function of P_S and P_B, is plotted in Figure 6 (left).

Validation of Analytical Calculation with Numerical Simulation

To validate the analytical calculation of *SNR* for SiPM, a numerical Toy Waveform Simulation was done. At a given P_S and P_B 1000 waveforms were simulated, and *SNR* was calculated as:

$$SNR_{sim.} = \frac{< A_S >}{\sigma_B} \tag{eq. 13}$$

where $<A_S>$ is an average detected laser signal amplitude and σ_B is noise standard deviation. An example of one simulated waveform (black) and overlap of 1000 waveforms together with $<A_S>$ and σ_B is presented in Figure 2.

The comparison of *SNR* from analytical calculation (i.e. Eq.11) and numerical waveform simulation is plotted Figure 3. We can observe a good agreement between simulation and analytical calculation at all simulated return laser power levels from 200 nW up to uW and background power levels from 0.1 pW up to nW. There is a small discrepancy at the lowest P_B = 0.1 pW. This difference could be related to SiPM microcell to microcell gain variation which is included in the waveform simulation but not in the analytical calculation.

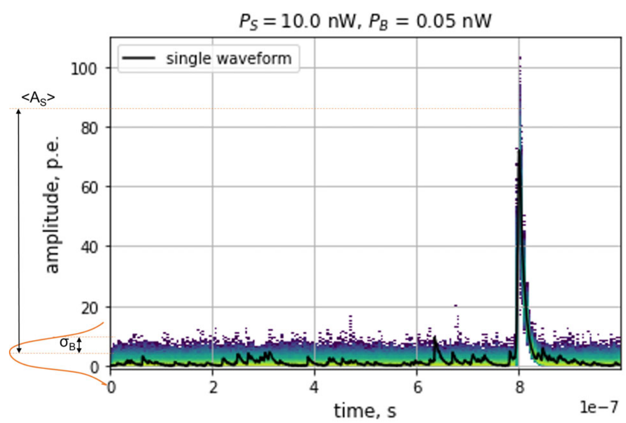

Figure 2. Collection of 1000 SiPM Waveforms Overlapped, and a Single Waveform (black line), simulated for P_B = 0.05 nW and P_S of 10 nW. Signal amplitude is expressed as number of detected single photon events (p.e.)

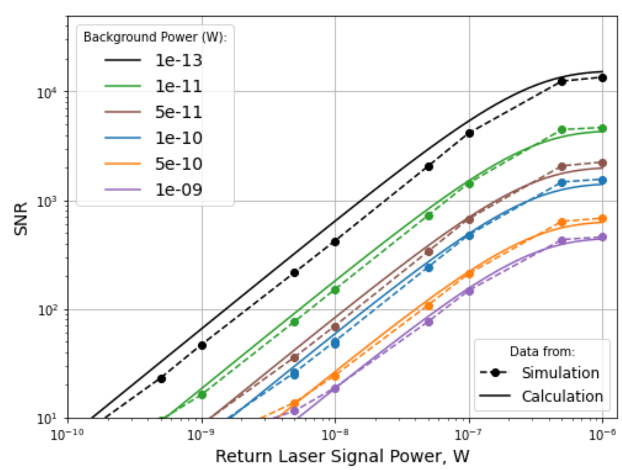

Figure 3. Comparison of *SNR* from Analytical Calculation (solid lines) and Numerical Simulation (dashed lines) under Various Background and Return Laser Signal Powers

Comparison of *SNR* for SiPM and APD

The *SNR* for onsemi SiPM and for APDs (Si and InGaAs), as a function of P_S and P_B, is plotted in Figure 6.

For comparison, the condition at which *SNR* = 10 is highlighted by red solid and dashed lines for SiPM, and APDs, respectively. The LiDAR detection probability P_D can be calculated for a selected *SNR* and false alarm rate. For example, P_D = 80% when *SNR* = 10 and false alarm probability, P_{fa} = 0.1% [5]:

$$P_D \approx 0.5 \times \mathrm{erfc}\left(\sqrt{-\ln(P_{fa})} - \sqrt{\mathrm{SNR} + 0.5}\right) \qquad \text{(eq. 14)}$$

The expected values of P_S and P_B are shown for three LiDAR test systems (Table 2) with variable receiver lens diameter D_{lens}.

We can observe that due to its single photon sensitivity the SiPM requires 14 times less return laser power with respect to the Si APD and 85 times less return laser power with respect to the InGaAs APD to achieve a *SNR* of 10 (SiPM requires 7×10^{-11} W, while Si APD needs 10^{-9} W and InGaAs 6×10^{-9} W).

Because of its high photon sensitivity, the onsemi SiPM is also more sensitive to ambient light. We can observe the effect of high background on *SNR* at $P_B > 10^{-12}$W for the SiPM, while the Si APD can tolerate two orders of magnitude higher $P_B \sim 10^{-9}$ W and the InGaAs APD is almost insensitive to ambient light level up to 10^{-7} W.

The *SNR* for those three systems is plotted in Figure 7. We can observe for the onsemi SiPM that *SNR* is limited by the high ambient light level when system *FoV* is 1°×1°. For Test System #2 with $AoV_x \times AoV_y$ = 0.1°×0.1° the SiPM−based system outperforms the APD−based system when Rx optics with small aperture are used (D_{lens} < 22 mm). Finally, for Test System #3 with $AoV_x \times AoV_y$ = 0.05°×0.05° the SiPM−based system outperforms both APD−based systems at any aperture (D_{lens}).

Effect of Read−out Electronics on *SNR*

The read−out electronics may affect performance in any light detection application. This model may also be used to analyze the effect of amplifier noise density $<V_{amp}>$ on *SNR*. The calculations were performed for SiPM and for Si APD with various values of feedback resistor R_f and noise bandwidth B_N because those parameters affect the *SNR* too. For InGaAs APD the effect is qualitatively similar to Si APD but quantitively even larger due to smaller *M*.

The *SNR* as a function of $<V_{amp}>$, calculated for different B_N and R_f is presented in Figure 4 and Figure 5 respectively for SiPM (left) and Si APD (right). The calculations were done at P_S = 1 nW and P_B = 0.07 nW where the SiPM and Si APD have the same *SNR* of 14. We can observe that for both SiPM and Si APD the *SNR* decreases with increasing $<V_{amp}>$ however the SiPM can tolerate almost two orders of magnitude higher $<V_{amp}>$ at the same B_N and R_f than APD due to higher internal Gain. Also, in the APD case the *SNR* shows much high dependence on B_N and R_f, while for SiPM the *SNR* is almost independent of B_N and R_f provided $<V_{amp}>$ stays below 10 nV/√Hz.

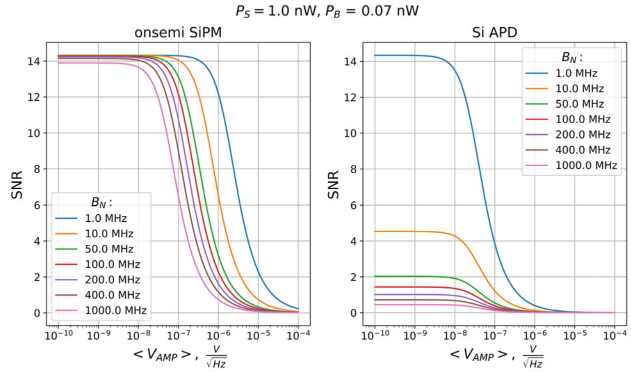

Figure 4. *SNR* as a Function of Amplifier Noise Density for SiPM (left) and Si APD (right) at Different B_N

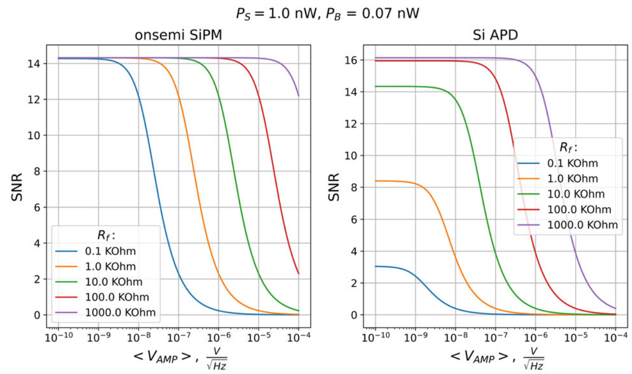

Figure 5. *SNR* as a Function of Amplifier Noise Density for SiPM (left) and Si APD (right) at Different R_f

SNR and Other LiDAR System Considerations

By comparing Si and InGaAs APD−based LiDAR systems, we observe that due to its higher internal noise (i.e., dark current I_D) and relatively low gain, *M*, **the InGaAs APD requires 5−7 times higher laser power to achieve the same *SNR* as the Si APD** under the same conditions (optics, resolution, background, sensor size.).

A system operating at 1550 nm is not constrained by the same eye safety power limit as a 905 nm system, which means the InGaAs APD−based system can compensate by using more powerful lasers. However, higher power laser means higher power consumption, more heat to be dissipated and, hence more bulky and less economical solutions.

Comparing the *SNR* for Si and InGaAs APDs and onsemi SiPM, one can observe that **due to its single photon sensitivity the onsemi SiPM requires 14 times less laser return power to achieve the same *SNR* as the Si APD and 84 times with respect to the InGaAs APD**.

While it is more sensitive to the light signal the SiPM is also more sensitive to ambient light compared to APDs. Therefore, the ambient light should be controlled to benefit from the advantages that the SiPM can provide. The background light power reaching the sensor can effectively be kept within the SiPM's operating range by using a small aperture lens and a narrow angular field of view. This is the case even under the high ambient light conditions that are encountered in automotive LiDAR.

These design solutions align well with existing trends in LiDAR system requirements i.e. miniaturization (small lens diameter) and high angular resolution (small angular field of view per SiPM).

It should be noted that a similar constraint would apply to the APD if it were to have a dramatically higher responsivity. In general, **a large aperture is recommended for LiDAR systems equipped with low light sensitivity detector or detector which could tolerate high ambient light level, while for systems equipped with high light sensitivity a small aperture size is preferable**.

A third consideration is the increasing use of VCSELs instead of classic edge−emitting lasers as illuminator. Due to having a smaller wavelength shift across operating temperature the **VCSEL enables the use of narrower bandpass filters on the Rx path**, which leads to ambient light reduction in the spectral regions adjacent to the wavelength of interest.

From analytical calculation of *SNR*, we found that due to relatively small internal multiplication *M*, **the choice of read−out electronics is critical for APD−based LiDAR system**, because the amplifier noise density could significantly reduce the *SNR*. To overcome this limitation and simplify the read−out electronics design, an APD with high *M* is required. Unfortunately, *M* is limited by APD dark current and could not exceed ~ 1k in the best scenario. This limitation is not a problem for SiPM devices which have much higher internal Gain of ~ 10^6. Such high gain allows the use of read−out electronics with almost two orders of magnitude higher noise density than APD−based systems can tolerate, without significant *SNR* degradation.

From Eq.7 and Eq.11 we observe that, independent of sensor type, $SNR \sim \sqrt{N_{shots}}$. Therefore, in either case, ***SNR* may be improved by a multi−shot approach**, taking multiple dToF measurements per point in the scene.

Summary and Takeaways

In this analysis we looked at analytical calculation of Signal to Noise ratio *SNR* for Si APD, InGaAs APD and **onsemi** SiPM sensors. The calculation was verified with a numerical waveform simulation for the SiPM case. We found that LiDAR systems could significantly benefit from the SiPM's single photon sensitivity and high internal gain for robust detection of low power return signals.

To realize all the advantages the SiPM could provide the optical system should be designed to suppress unwanted interference from ambient background light. In practice this leads to optical system miniaturization and high angular resolution

Also, due to its much higher internal Gain, the SiPM−based LiDAR system will tolerate almost two orders of magnitude higher noise density in the readout chain than APD−based systems, without significant *SNR* degradation, making the SiPM−based system less dependent on readout performance, and thus simplifying the readout design task.

In conclusion, by utilizing SiPM sensors instead of APD in 905 nm LiDAR the detection range can be increased, or the laser power can be reduced while simplifying readout electronics and optimizing the optical system, making the SiPM better suited to achieving low cost, low power, and compact LiDAR solutions.

For more information about SiPM for LiDAR go to onsemi.com/support

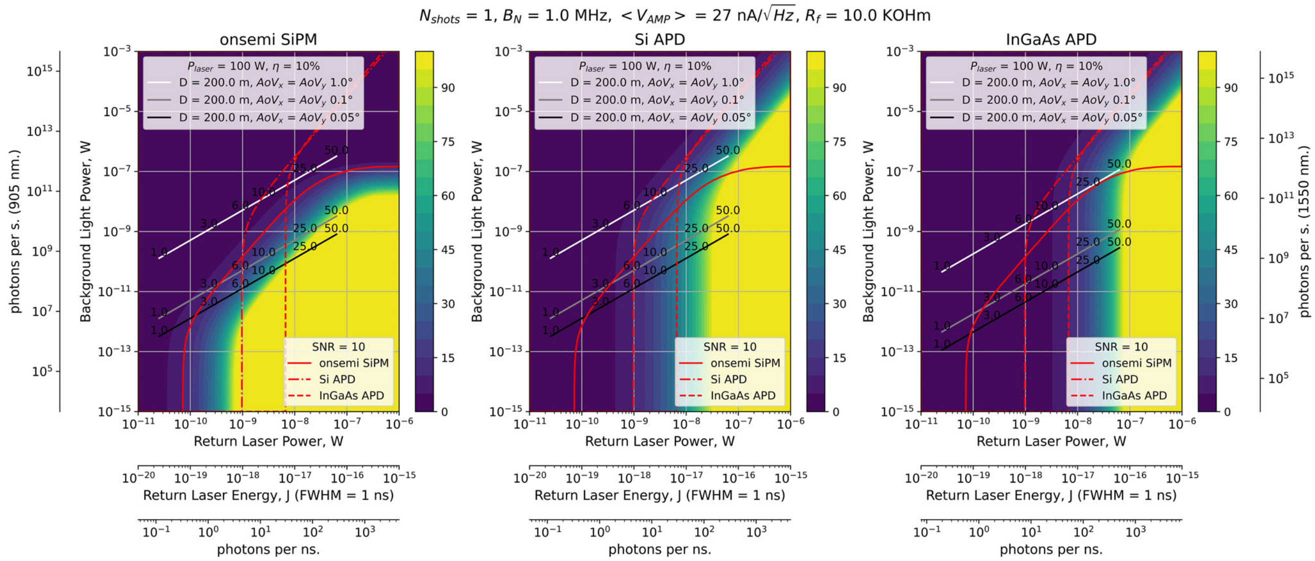

Figure 6. *SNR* for onsemi SiPM (left), Si APD (middle) and InGaAs APD (right) as a Function of P_S and P_B. The red lines represent *SNR* = 10. The expected value of P_S and P_B for target with η = 10% at 200 m distance, for different D_{lens} from 1 to 50 mm, and different *AoV* are presented by white ($AoV_x \times AoV_y$ = 1° × 1°), grey ($AoV_x \times AoV_y$ = 0.1° × 0.1°) and black ($AoV_x \times AoV_y$ = 0.05° × 0.05°) lines. The *SNR* was limited to 100.

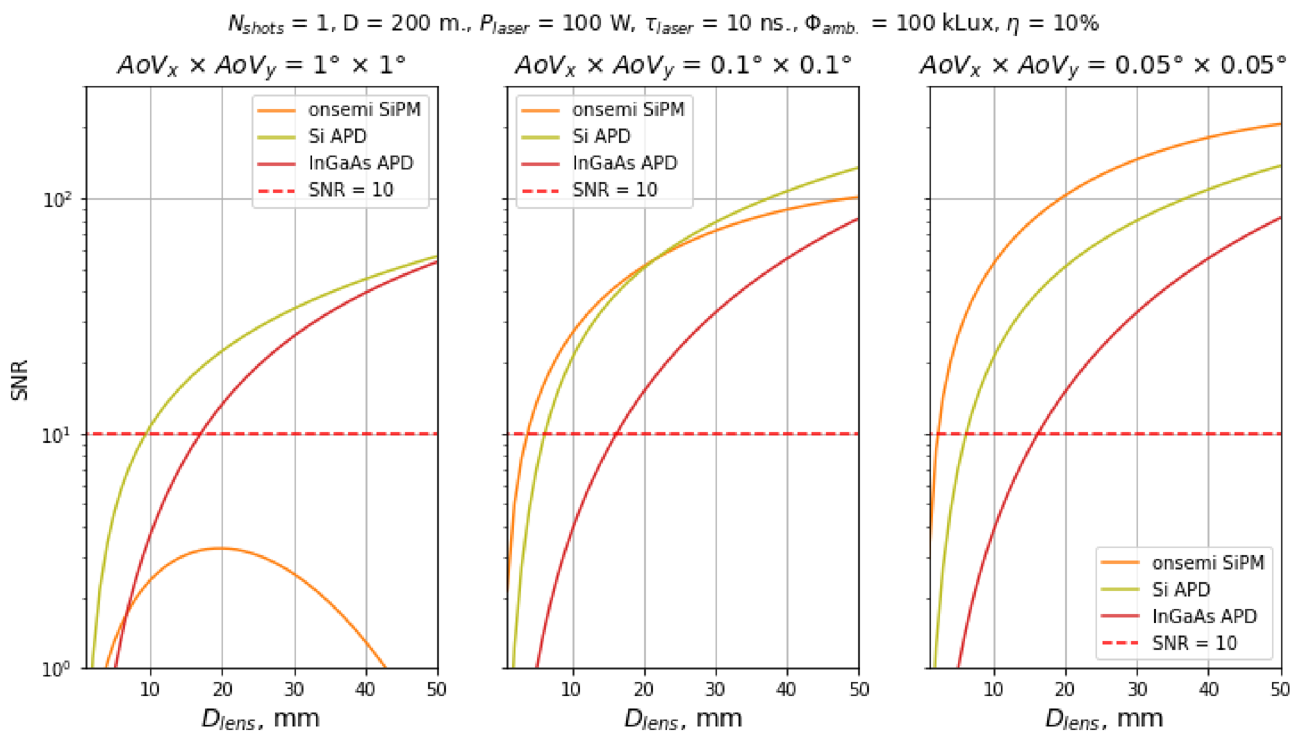

Figure 7. *SNR* as a Function of Rx Lens Diameter, D_{lens}, for Three Test Systems (for test system details, refer to Table 2) with different Field of View per channel (i.e. resolution). Results presented for onsemi SiPM (orange), Si APD (olive) and InGaAs APD (red) (sensor specifications are presented in Table 3). The red dashed line represents the reference point where *SNR* = 10.

References

[1] S. Gnecchi and C. Jackson, “A 1 × 16 SiPM Array for Automotive 3 D Imaging LiDAR Systems,” 2017.

[2] A. Buchner, S. Hadrath, R. Burkard, F. Kolb, J. Ruskowski, M. Ligges and A. Grabmaier, “Analytical Evaluation of Signal−to−Noise Ratios for Avalanche− and Single−Photon Avalanche Diodes,” *Sensors,* vol. 21, p. 2887, 2021.

[3] **onsemi**, “Introduction to the Silicon Photomultiplier (SiPM) AND9770/D,” 08 2023. [Online]. Available: https://www.onsemi.com/download/application−notes/pdf/and9770−d.pdf.

[4] S. Vinogradov, “Analytical models of probability distribution and excess noise factor of Solid State Photomultiplier signals with crosstalk,” *NIM A,* vol. 695, 2012.

[5] D. Chu, S. Aboujja and D. Bean, “1550nm triple junction laser diode for long range LiDAR,” *inproceedings,* p. 23, 2022.